Diagnostic and Interventional Imaging (2014) **95**, 1055—1063

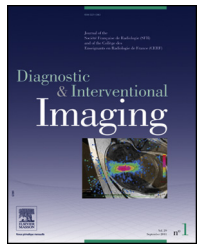

ORIGINAL ARTICLE / *Genito-urinary imaging*

Renal papillary carcinoma: CT and MRI features

C. Couvidat [a], D. Eiss [a,*], V. Verkarre [b], S. Merran [c], J.-M. Corréas [a], A. Méjean [d,e], O. Hélénon [a]

[a] *Department of Adult Radiology, Necker Hospitals, Paris Public Hospitals Health Service, 149, rue de Sèvres, 75015 Paris, France*
[b] *Department of Pathological Anatomy, Necker Hospitals, Paris Public Hospitals Health Service, 149, rue de Sèvres, 75015 Paris, France*
[c] *Léonard-de-Vinci Medical Imaging, 43, rue Cortambert, 75016 Paris, France*
[d] *Department of Urology, Necker Hospitals, Paris Public Hospitals Health Service, 149, rue de Sèvres, 75015 Paris, France*
[e] *Georges-Pompidou European Hospital, Paris Public Hospitals Health Service, 20, rue Leblanc, 75015 Paris, France*

KEYWORDS
Kidney;
Papillary renal cell carcinoma;
Renal cancer;
CT;
MRI

Abstract
Purpose: To describe the CT and MRI appearances of papillary renal cell carcinoma.
Materials and methods: Retrospective study of 102 papillary carcinomas in 79 patients, 81 tumors examined by CT and 56 by MRI. Tumor size, homogeneity and contrast enhancement were recorded.
Results: The most common presentation of papillary renal cell carcinoma was a small homogeneous hypovascular tumor both on CT and MRI. Eighty-nine percent of lesions were hypointense on T2 weighted images compared to the renal parenchyma. Seventeen percent of the lesions did not significantly enhance with contrast on CT. All of the lesions examined on MRI had a significant enhancement percentage. Calcifications were rare and only seen in 7% of cases (CT). The second most common presentation was a bulky necrotic tumor. In addition, atypical types of disease were found which were difficult to diagnose, including infiltrating tumors and tumors with a fatty component.
Conclusion: A homogeneous hypovascular renal tumor which is hypointense on T2 weighted images should suggest a diagnosis of papillary carcinoma. Some papillary carcinomas do not enhance significantly on CT. MRI is then required to diagnose the renal tumor.

Abbreviations: PC, Papillary carcinoma; CCC, Clear cell carcinoma; CT, Computed tomography; MRI, Magnetic resonance imaging; PACS, Picture Archiving and Communication System; HU, Hounsfield unit; ROI, Region of interest; PI/OP, In phase/out of phase; AML, Angiomyolipoma.

* Corresponding author.
E-mail address: david.eiss@nck.aphp.fr (D. Eiss).

http://dx.doi.org/10.1016/j.diii.2014.03.013
2211-5684/

Introduction

Papillary carcinoma (PC) accounts for 10 to 15% of renal cell carcinomas [1]. There have been many difficulties over several years in classifying this tumor according to its histological and cytogenetic features [1] (classification into types 1 and 2 [2,3], carcinomas with MITF/TFE translocations, tubulomucinous carcinomas, etc.). Its prognosis compared to clear cell carcinoma (CCC) has been extensively debated: the ''conventional'' assumption that PC carries a better prognosis [4—7] has been contested, as studies [8,9] on large series have concluded that both histological subtypes carry a similar prognosis for the same stage and grade. Because papillary carcinomas are often multifocal and bilateral, their preoperative diagnosis is important and may lead to treatment to preserve the kidney, particularly as the current indications for partial nephrectomy are widening and percutaneous ablation techniques (radiofrequency and cryoablation) are increasingly being used.

Current findings reported in the literature suggest that the tumor is often hypovascular on computed tomography (CT) [10] and MRI [11], and is hypointense on T2 weighted imaging [11]. We have reviewed the sectional imaging of 102 tumors in order to examine the most typical features of papillary renal cell carcinoma and to identify misleading appearances which can lead to diagnostic errors.

Materials and methods

Study population

The patients were selected from pathological anatomy and radiological databases.

We searched for any CT and MRI investigations performed before surgery or biopsy. The investigations had to be available on the imaging system (Picture Archiving and Communication System [PACS]) in order to enable the various measurements to be performed (investigations which were only available on film were not included). Only tumors at least 10 mm in size were considered (microlesions under 10 mm in size were excluded in order to avoid partial volume effects when density and signal measurements were made and the stiffening effect of the CT beam [12]).

Pathological anatomy examination (surgical specimen or biopsy) was available for each patient and included both a macroscopic examination (for surgical specimens) and histology (hematoxylin-eosin-safran staining). Immunohistochemistry (in particular, anti-cytokeratin 7 antibodies, vimentin, racemase and CD 10) were performed on some tumors.

One hundred and two papillary carcinomas were found over a period of 6 years (between 2002 and 2008) in 79 patients (60 men, 19 women, sex ratio = 3.2). The average age of the patients was 61 years old (with a range of 18 to 84 years old).

CT technique

We found 81 tumors which were investigated by computed tomography using a 4-stage protocol in 75% of cases (61 patients): unenhanced, and then in the arterial phase (30 to 40 seconds after beginning the iodine contrast injection), tubular phase (90 to 120 seconds) and delayed phase (between 3 and 6 minutes), on a 4 detector helicoidal machine, Philips Mx 8000 (Marconi Medical System). All but two of the remaining 25% of patients had a 3-stage CT investigation (involving helicoidal acquisition without enhancement and then in the arterial and delayed phases), performed on an Aquilion 16 detector helicoidal machine (Toshiba).

The contrast medium used was Xénétix 350, injected intravenously into the brachial vein in the antecubital fossa (120 to 140 mL, not exceeding 2 mL/kg patient body weight; injections rate: 2.5 to 3.5 mL/s). The following features were recorded for each lesion:

- topography: number of tumors, site, size (2 perpendicular measurements in the axial plane);
- morphology: encapsulated appearance (a tumor with well demarcated boundaries deforming the contour of the kidney with a mass effect on adjacent structures) or infiltrating (poorly demarcated tumor boundaries not deforming the outline of the kidney but occasionally increasing its volume with invasion of adjacent structures); calcifications; fatty component (density less than −20 HU) within the tumor; homogeneity after iodine contrast enhancement;
- measurement of density: density in Hounsfield units (HU) before the injection and in the different stages: maximum enhancement (maximum density − density before injection); acquisition time at which the enhancement was maximal;
- locoregional extension: invasion of the renal vein; enlarged lymph nodes.

MRI technique

We found 56 tumors examined by MRI (Genesis Signal HD 1.5 T machine, General Electric Healthcare) in 38 patients. The protocol involved a single plane, usually axial (and occasionally coronal, depending on the site of the lesion), T2 weighted images with fat suppression (Fat Sat) (RT: 6,000 to 8,000 ms; ET: 90 to 106 ms), T1 weighted images (RT: 165 to 200 ms; ET: 1.5 to 1.9 ms) and a T1 weighted 3D EG ultrarapid dynamic image before and after injection of gadolinium chelate (Dotarem, 0.2 mL/kg patient body weight, 2 mL/s) in the arterial phase (30 seconds after beginning the injection), tubular phase (90 seconds) and delayed phase (3 to 6 minutes with a sequence at 10 minutes in some cases). In phase and out of phase images (IP/OP) were also available in 34% of patients (19 of 56 tumors). The following MRI features were examined:

- topography: number of tumors; site; size (two perpendicular measurements);
- morphology: encapsulated or infiltrated appearance; tumor appearance on T1 and T2 Fat Sat weighted images compared to the adjacent renal parenchyma; homogeneity; qualitative comparison of tumor image between in phase and out of phase images;
- examination of contrast enhancement: measurement of the tumor image on the dynamic sequence in the different phases; calculation of percentage enhancement ((max signal − signal without enhancement)/signal without enhancement × 100), which was defined as positive if

it was over 15% [13] and the acquisition time at which the enhancement was maximal;
- locoregional extension: invasion of the renal vein; enlarged lymph nodes.

Thirty-five tumors were studied using both methods.

The regions of interest (ROI) were identified both on CT and on MRI:
- for homogeneous lesions: in the central part of the tumor;
- for cystic/necrotic lesions: in the tissue part of the portion of the lesion if this was of sufficient size.

The ROI were identical in size and position in all phases.

Results

Topography

Seven patients (9%) had multiple tumors, including 2 (2.5%) who had bilateral tumors. The tumor was located in the right kidney in 53% of cases and in the left kidney in 47% of cases. In 4% of cases, the tumor had developed in the patient's natural kidney in a renal transplant patient.

CT

Morphology

The tumors were encapsulated in 98% of cases. Two tumors were infiltrating.

The tumor had developed in the cortex in 97% of cases.

The lesions were homogeneous in 85% of cases and had an average size of 2.4 cm (from 1.0 to 7.7 cm) (Fig. 1) compared to an average size of 10.1 cm (from 6.8 to 18.4 cm) in the 15% of tumors which had heterogeneous enhancement and contained a cystic or necrotic proportion (Fig. 2). Six tumors (7% of tumors examined on CT) contained calcifications. Half of these were peripheral and linear and half were rounded in appearance (Fig. 3).

One tumor contained a fatty density (density less than −20 HU), because of bone metaplasia (Fig. 4). This tumor also contained calcifications. These findings are summarized in Table 1.

Density and contrast enhancement

Mean tumor density before enhancement was 35 HU (from 10 to 62 HU).

It was not possible to calculate the maximum enhancement in two cases as there was no unenhanced phase. The percentages below were therefore calculated from a total of 79 tumors.

The distribution of maximum enhancement values is shown in Fig. 5.

Variation in density was indeterminate in 16.5% of cases (between 10 and 15 HU) or negative (less than 10 HU) in 5% of cases. These were small lesions (on average 29 mm along their long axis, with a range of 12 to 43 mm) which were homogeneous and not calcified (Fig. 6). Their average density before enhancement was 31 HU, with a range of 10 to 45 HU. In two cases the unenhanced density was less than

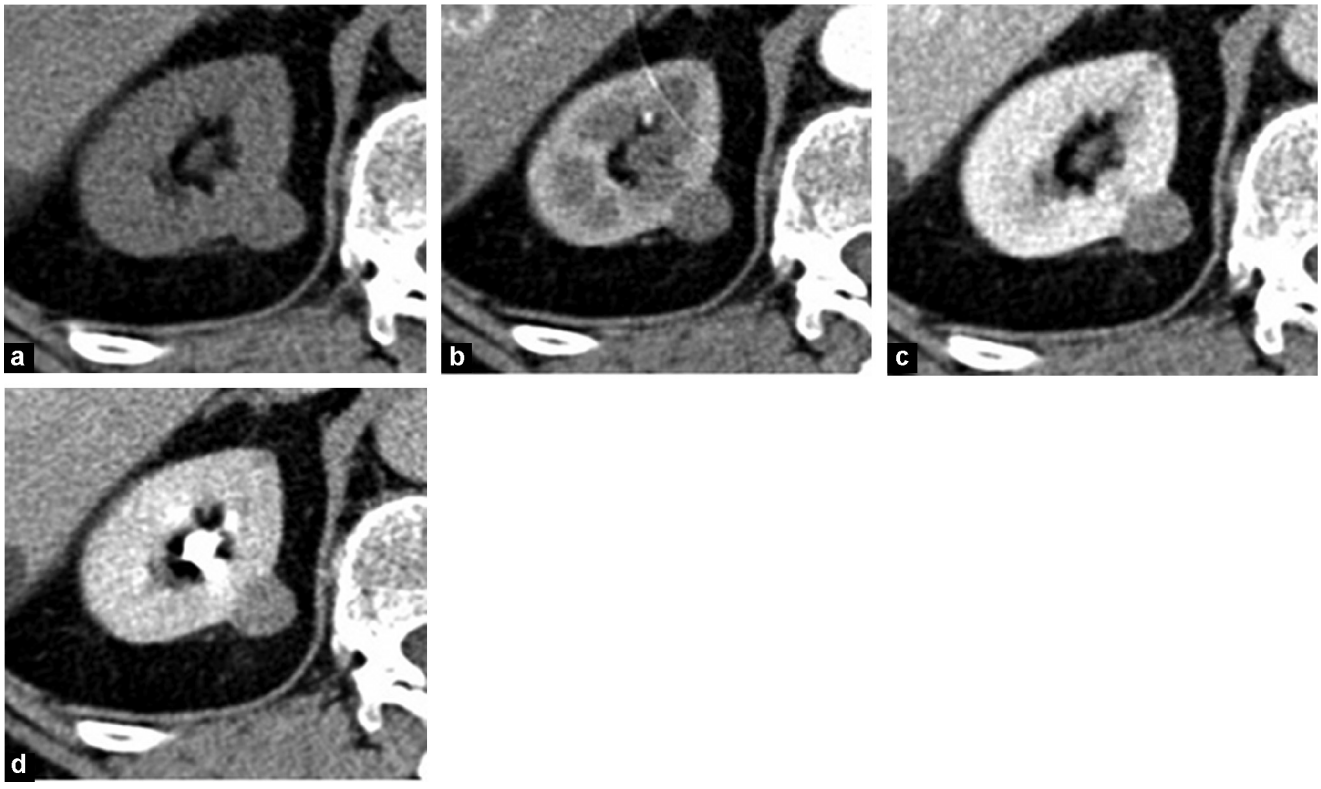

Figure 1. Small clearly demarcated, homogenous tumor enhancing weakly: typical CT appearance of papillary carcinoma; a: unenhanced (33 HU); b: arterial phase (38 HU); c: tubular phase (62 HU); d: delayed phase (66 HU).

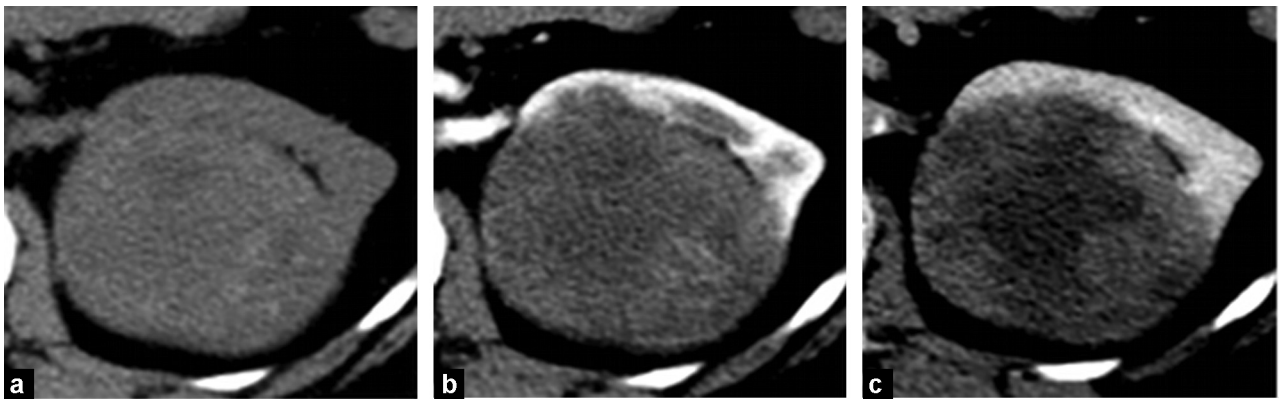

Figure 2. Massively necrotic heterogeneous papillary carcinoma. CT: a: before enhancement; b: arterial phase; c: tubular phase.

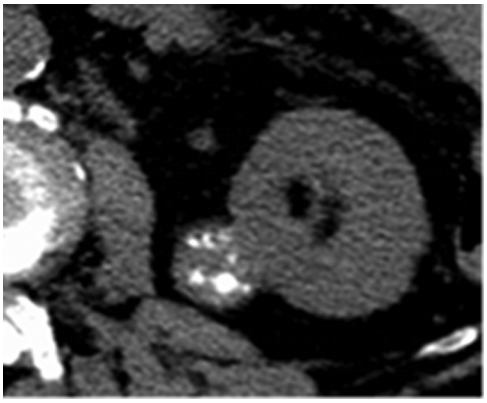

Figure 3. Papillary carcinoma with multiple rounded calcifications. Unenhanced CT.

20 HU. The maximum contrast enhancement in these two lesions was 14 and 15 HU, respectively.

Maximum enhancement was less than 40 HU in 82% of cases.

If only the small tumors under 3 cm in size were considered, 100% of lesions were homogeneous and average maximum contrast enhancement was 35 HU (from 13 to 91 HU).

The time to maximum enhancement was recorded for the tumors which were examined using a 4-phase protocol. This was during the tubular phase in 67%, followed by the delayed phase (22%) and arterial phase (11%) (Fig. 7).

Locoregional invasion

The two infiltrating tumors were associated with renal vein invasion. There were also necrotic enlarged retroperitoneal lymph nodes (peri-hilar and inter-aorta-caval regions) in one case (Fig. 8), which was a sarcomatoid form of papillary carcinoma (Fuhrman high grade).

MRI

Morphology

The T2 weighted tumor signal was homogeneous in 57% of cases, slightly heterogeneous in 9% and heterogeneous in 34%.

Eighty-nine percent of tumors were hypointense compared to the normal renal parenchyma on T2 weighted images (Fig. 9), 9% were hyperintense and 2% were isointense.

Tumors under 3 cm in size (48%) were all hypointense on T2 weighted images.

The tumor signal was more variable on T1 weighted images: 50% were isointense, 32% were hypointense and 18% were hyperintense.

Of the tumors examined using in phase and out of phase (IP/OP) sequences, 47% (9/19) had a lower in phase signal intensity than out of phase. This was diffuse in 6 cases

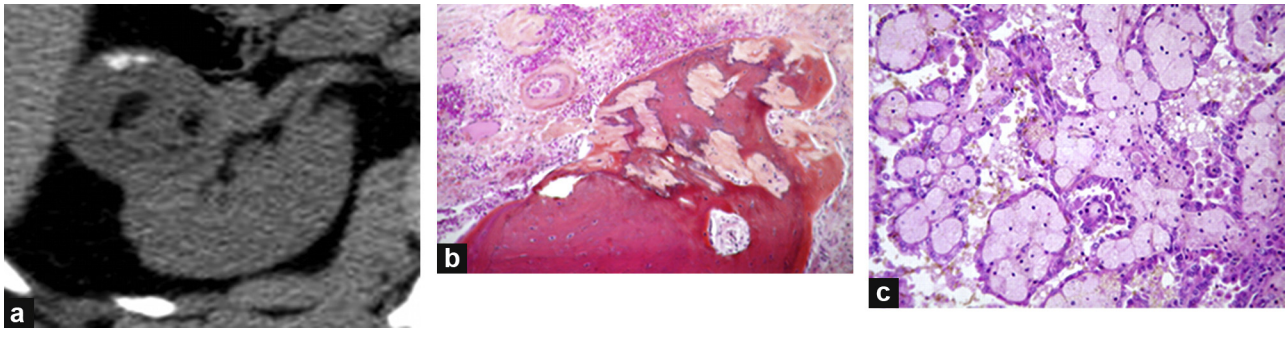

Figure 4. Papillary carcinoma containing an area of fatty density combined with calcifications; a: unenhanced CT; b: histology: HES staining magnification × 4. Area of bone metaplasia calcified in placed representing the macroscopic area of fat seen on the CT; c: histology: HES staining magnification × 20. Tumor of papillary architecture with foamy macrophages along the axes bordered by a layer of tumor cells.

Table 1 Topographic, morphological and locoregional extension features on CT and MRI.

Features	Number of tumors involved (percentage)
Topography	
Multiple tumors	7 patients (9%)
Bilateral tumors	2 patients (2.5%)
Type of tumor	
Encapsulated	100 (98%)
Infiltrating	2 (2%)
CT features	
Homogeneous (mean size: 2.4 cm)	69 (85%)
Heterogeneous (mean size: 10.1 cm)	12 (15%)
Calcifications	6 (7%)
Macroscopic fatty component	1 (1%)
MRI features	
T2	
Homogeneous	32 (57%)
Slightly heterogeneous	19 (34%)
Heterogeneous	5 (9%)
T2	
Hypointense	50 (89%)
Isointense	1 (2%)
Hyperintense	5 (9%)
T1	
Hypointense	18 (32%)
Isointense	28 (50%)
Hyperintense	10 (18%)
IP/OP	
Increased in out	9/19 (47%)
Fall in out	3/19 (16%)
No change	7/19 (37%)
Locoregional extension	
Invasion of veins	2 (2%)
Enlarged lymph nodes	1 (1%)

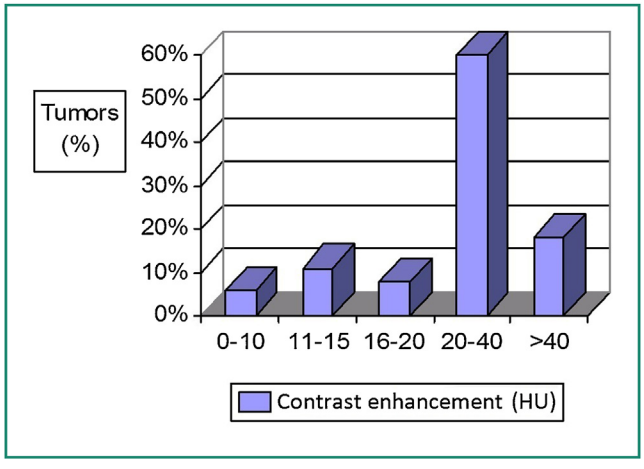

Figure 5. Histogram showing the distribution of maximum contrast enhancement on CT.

(Fig. 10) and focal in the other 3 cases. In three tumors (16%), the signal intensity was lower on the out of phase sequence.

These findings are summarized in Table 1.

Study of contrast enhancement

The average contrast enhancement percentage, which was defined as significant over 15% [13], was 68% (range from 16 to 278%). All of the tumors enhanced significantly. Contrast enhancement was 80% or less in 78% of cases.

Nine of the 13 tumors which did not enhance significantly on CT were examined by MRI. All of these enhanced significantly with an average contrast enhancement of 48% (from 25 to 74%).

Mean contrast enhancement in the tumors under 3 cm in size was 69% (from 20 to 172%).

The distribution of maximum enhancement times was similar to what was found on CT (Fig. 7): 60% of tumors exhibited maximum enhancement on the tubular phase, 30% on the delayed phase and 10% on the arterial phase.

Locoregional invasion

One infiltrating tumor was associated with invasion of the renal vein and enlarged necrotic lymph nodes (the sarcomatoid form of papillary carcinoma which was examined on both CT and MRI).

Discussion

The histological classification of renal cell carcinomas is based on histological, immunohistochemical and cytogenetic features.

Several studies have been carried out in order to distinguish histological types on CT [14,15] and MRI [11,16].

The ''encapsulated form'', i.e. tumors with well demarcated boundaries deforming the contours of the kidney and pushing back adjacent structures, made up 98% of the tumors in our series. Infiltrating tumors are rare amongst the papillary carcinomas and in the ''common'' renal cell carcinomas in general (clear cell, papillary and chromophobe cell carcinomas) where they usually represent high Fuhrman grade and more aggressive sarcomatoid tumors [17]. The infiltrating lesions are usually due to urothelial carcinomas of the pyelocaliceal cavities, hemopathies (lymphomas or leukemias), rare renal cell carcinomas (collecting duct carcinomas, renal medullary carcinomas) or inflammatory lesions (xanthogranulomatous pyelonephritis or malakoplakia) [18–20].

Only 7% of the lesions in our series contained calcifications. This is less than is reported in the literature, which describes 23% [15] or even 32% [14] of PC as being calcified. These figures are possibly overestimated as the series involved small numbers of tumors (26 and 19 PC respectively).

One tumor contained an area of fatty density, i.e. a density of less than −20 HU on the unenhanced image, because of bony metaplasia. The presence of a macroscopic fatty component in a renal mass should suggest the diagnosis of angiomyolipoma (AML), a benign tumor which, depending on its size, requires surveillance or treatment (embolization or

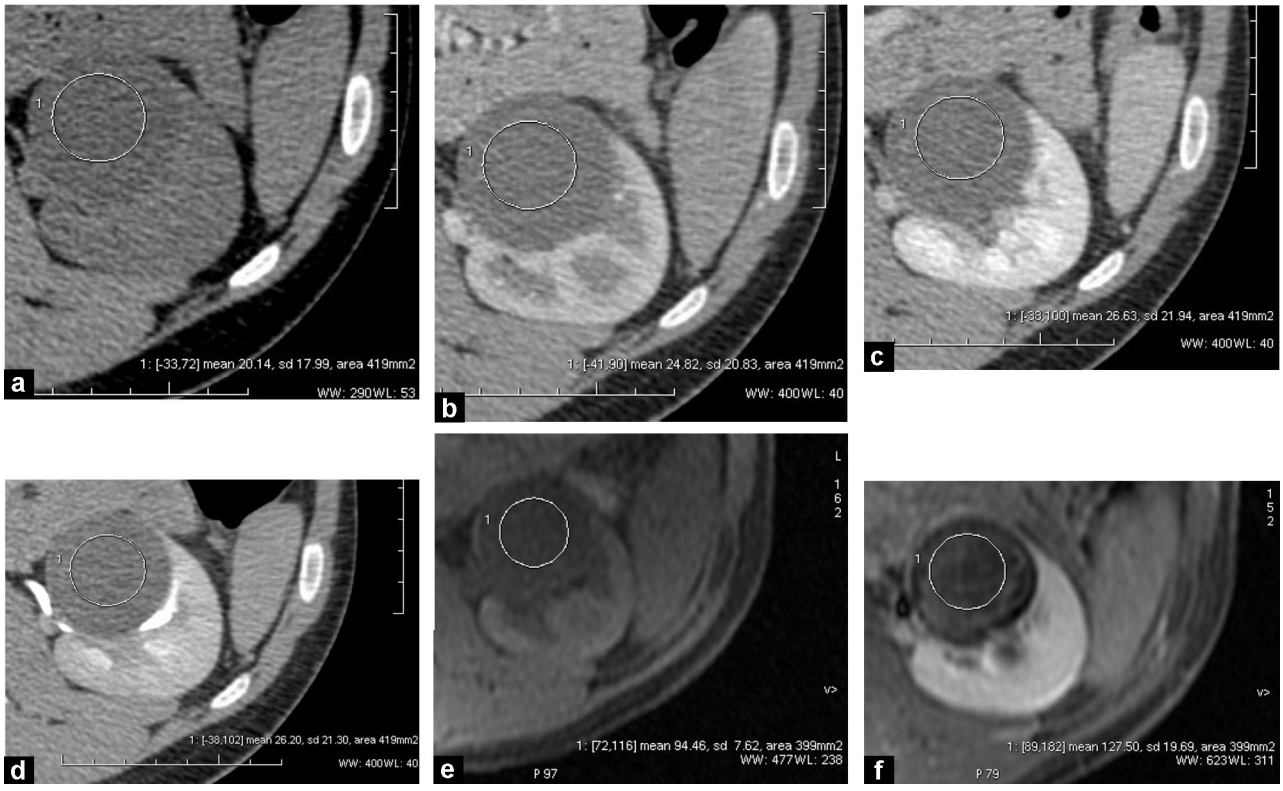

Figure 6. Papillary carcinoma without enhancement (7 HU difference between the tubular phase and pre-enhancement image), exhibiting significant contrast enhancement on MRI (36% enhancement); a: unenhanced CT; b: CT: arterial phase; c: CT; tubular phase; d: CT: delayed phase; e: MRI: T1 weighted image without enhancement; f: MRI: T1 weighted image in the delayed phase.

surgery). The case described in our series also contained calcifications. The diagnosis of AML should be reconsidered if calcifications are combined with an area of fatty density in a renal tumor, as calcified AML are extremely rare [21]. Conversely, malignant tumors (including papillary carcinomas) containing macroscopic fat are described in the literature [22—24]. There are four possible mechanisms to explain this: bony metaplasia (with islets of fatty bone marrow), massive necrosis with the formation of amalgams of lipids from cells, cholesterol necrosis and ''trapping'' of perirenal fat or fat inside the sinuses [23].

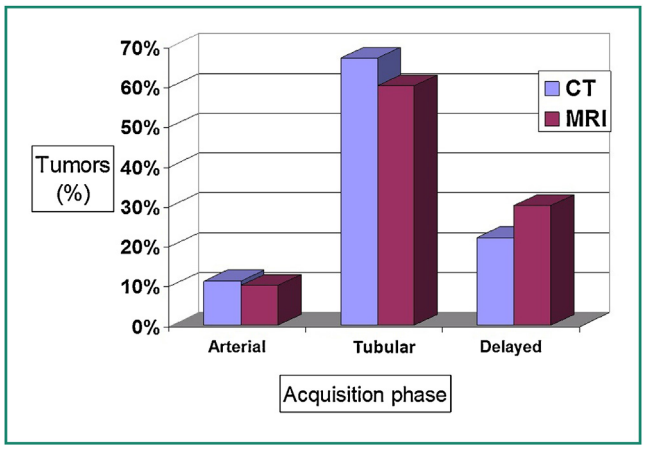

Figure 7. Histogram showing the distribution of maximum contrast enhancement by investigation time on CT (for tumors examined using a 4 acquisition protocol) and on MRI.

Cases of renal cell carcinoma containing fat without concomitant calcifications have been described in the literature [25]. It is far more difficult to diagnose a malignant tumor in these situations, although some signs do suggest malignancy, including a bulky tumor with irregular outlines invading the perirenal or sinus fat, a bulky necrotic tumor containing small areas of fat or signs of malignancy, such as invasion of veins or enlarged lymph nodes [24].

One of these mechanisms, cholesterol necrosis, is specific to PC as one of the histological features of PC is that it contains foamy macrophages located along the axis of the papillae. If these macrophages are saturated with cholesterol crystals they may become necrotic and extracellular cholesterol deposits develop. The signs which suggest PC with cholesterol necrosis in a tumor containing a macroscopic area of fat but no calcifications are a bulky tumor with low (tumor/healthy parenchyma ratio less than 25% in the arterial phase) but homogeneous enhancement (except in the areas of fat) [22].

In 16.5% of tumors, there is no significant enhancement on CT (less than 15 HU) and this may lead to a tumor being missed. The tumor density before enhancement should alert the radiologist to the diagnosis.

With only two exceptions, all of these lesions were of non-liquid density (over 20 HU) before enhancement and therefore did not meet the diagnostic criteria for a simple cyst (type 1 of the Bosniak classification [26]). They also did not meet the diagnostic criteria of a type 2 cyst (high

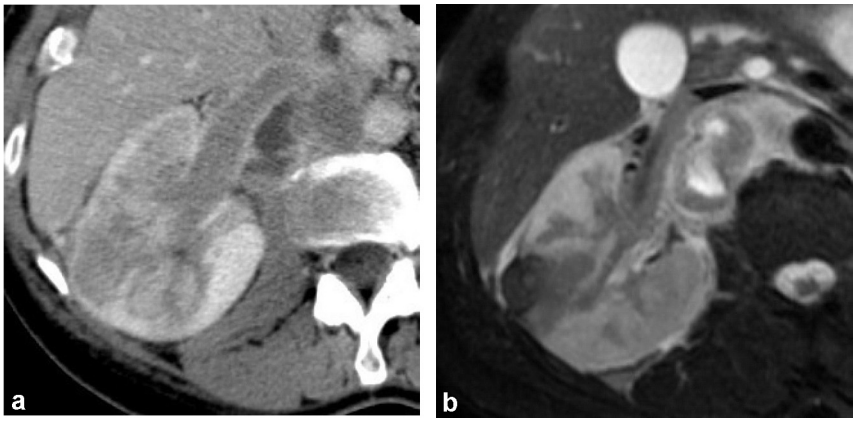

Figure 8. Infiltrating, sarcomatoid, papillary carcinoma with invasion of the renal vein and enlarged necrotic retroperitoneal lymph nodes; a: CT: tubular phase; b: MRI: T2 weighted image.

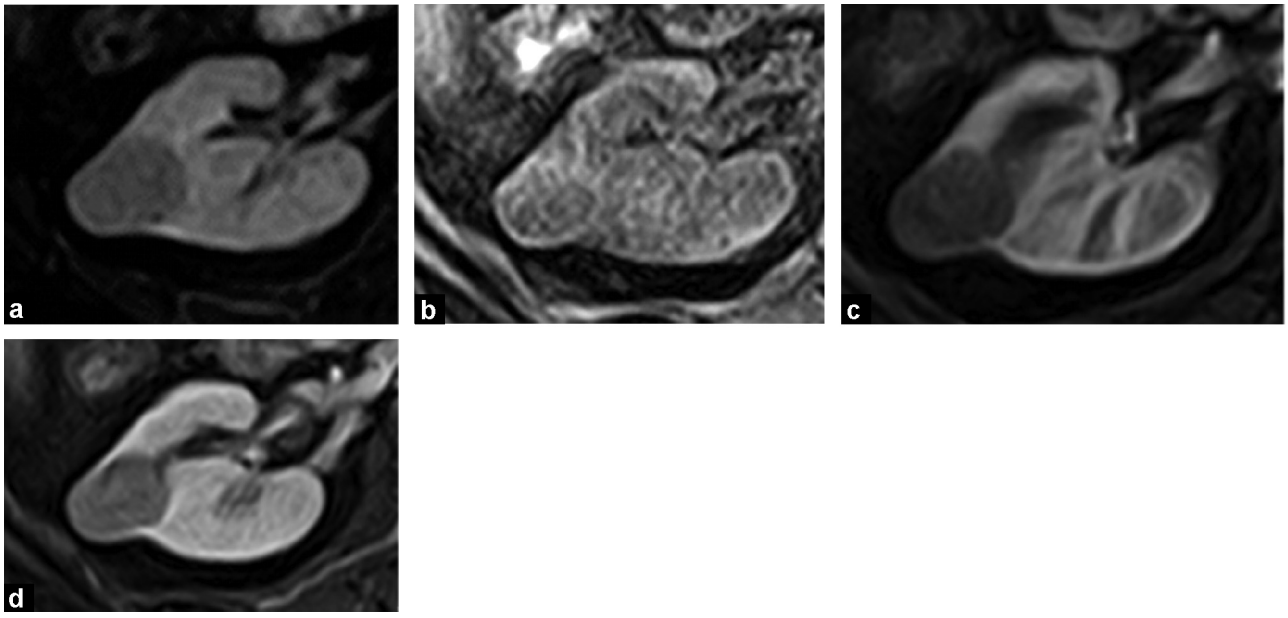

Figure 9. Typical MRI appearance of a papillary carcinoma: small homogeneous, well demarcated tumor, hypointense on T2 weighted image, enhancing weakly (65%) but significantly; a: MRI: T2 weighted image; b: MRI: unenhanced T1 weighted image; c: MRI: T1 weighted image, arterial phase; d: MRI: T1 weighted image, tubular phase.

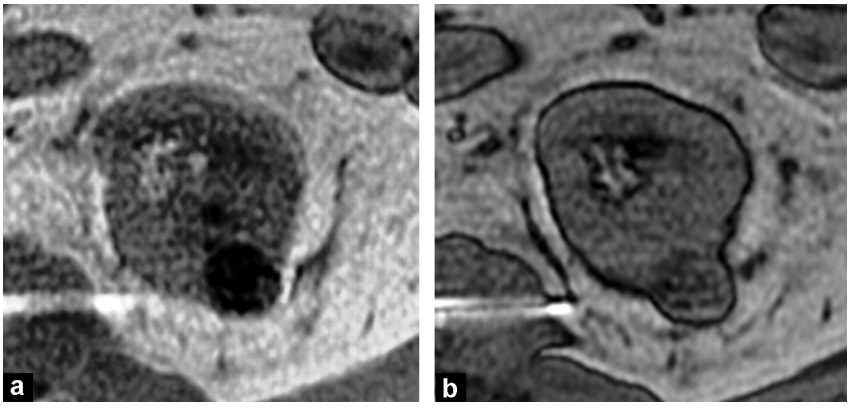

Figure 10. Papillary carcinoma with reduced in phase signal; a: MRI: in phase image; b: MRI: out of phase image.

attenuation cyst) as their pre-enhancement density was less than 50 HU. These were therefore isodense renal parenchymal lesions which did not take up the contrast significantly on CT and cannot therefore be diagnosed by CT and require MRI. The two lesions with a density of less than 20 HU before enhancement (and which were therefore ''pseudo-liquid''), changed in density by 14 and 15 HU respectively. The change in density after enhancement was therefore indeterminate and required MRI to distinguish a cyst (which may be simple, protein rich or hemorrhagic) from a hypovascular tumor [27].

When Bosniak's criteria are used to define whether contrast enhancement is present [28], 24% of lesions had negative (0 to 10 HU: 6% of tumors) or equivocal contrast uptake (10 to 20 HU: 18%).

The lack of significant contrast enhancement on CT may be related to the histological type of tumor as 10 (77%) of the 13 tumors (16.5%) which did not significantly enhance on CT were type 1 PC. In addition, 8 of these tumors had been examined using a 4-phase protocol (without enhancement, arterial, tubular and delayed) and maximum enhancement was found in the tubular phase in all of these cases. This does not support the hypothesis that a later acquisition (after 6 minutes) can identify a significant contrast enhancement.

As the activities at the Necker Hospital are focused on urological oncology, our study may suffer from recruitment bias, with a larger number of tumors which have an atypical or difficult radiological presentation. This may partly explain the large number of tumors which did not take up contrast in CT, some of which were incorrectly reported as cystic lesions in previous investigations.

Ninety-seven percent of tumors enhanced in the arterial phase below the cut off of 84 HU. This is consistent with the study report by Kim et al. [14] designed to distinguish clear cell carcinomas from other histological types of tumor.

One of the weaknesses of our series is that because it was retrospective, there was a degree of variation in the number of CT acquisitions in our cases (from two to four) and in the contrast medium used (osmolality, amount, flow rate) which are technical parameters that influence the measured densities [29].

On MRI, the papillary carcinoma was hypointense on T2 weighted images in 89% of cases which is consistent with findings published in the literature [11,30].

Papillary carcinoma also appears as a hypovascular tumor with a mean enhancement percentage of 68 and 69% for tumors under 3 cm in size, less than the figures reported by Roy et al. [11] (120% in a series of 55 papillary carcinomas under 3 cm in size) and by Sun et al. [16] (from 93 to 113% depending on Furhman grade, on 28 papillary carcinomas).

MRI is more sensitive on contrast enhancement than CT. Nine of the 13 tumors which did not significantly enhance with contrast on CT were also examined by MRI and in 100% of these cases contrast enhancement was significant. MRI is therefore indicated if any doubt remains about the type of tissue involved in the renal lesion on CT.

Ninety-one percent of the lesions met the diagnostic criteria defined by Sun et al. [16] for the differential diagnosis between papillary carcinoma and clear cell carcinoma, i.e. arterial phase enhancement of less than 84% on MRI.

Increased signal on an out of phase image compared to the in phase image may be an additional diagnostic feature supporting papillary carcinoma on MRI. This was present in 47% (9/19) of lesions in our series and was reported in 44% of papillary carcinomas compared to 14% of clear cell carcinomas in a study on 9 papillary carcinomas and 57 clear cell carcinomas [31]. The increased signal on the out of phase image may be due to hemosiderin within the tumor [31], a common feature of papillary carcinomas [32]. One study published in 2009 [33] reported that hemosiderin was present as commonly in papillary carcinomas (38% of cases) as in clear cell carcinomas (44%). Further studies are needed to confirm the diagnostic value of the hypointensity on the in phase image in papillary carcinomas compared to other histological types of renal tumors, particularly clear cell carcinomas.

It may be useful to distinguish between these two histological types on imaging particularly in higher risk surgery patients or patients with a familial form of papillary carcinoma who can be offered alternative treatments to surgery (particularly percutaneous radiofrequency ablation).

Conclusion

Papillary carcinoma typically presented as a small, homogeneous, hypovascular, uncalcified tumor which was hypointense on T2 weighted sequences in our series. A significant proportion of tumors (17%) did not enhance significantly on CT. These forms of tumor were usually of the same density as the adjacent renal parenchyma before enhancement and should not be interpreted as cystic lesions. If any doubt remains, MRI should be performed as it is more sensitive to contrast enhancement (all of the lesions which did not enhance significantly on CT which were investigated by MRI significantly enhanced on a T1 weighted dynamic image after gadolinium).

Tumors which appear cystic or necrotic are not rare and in this case it is more difficult to diagnose a papillary carcinoma from another histological type of tumor, particular clear cell carcinoma with a necrotic component.

Finally, atypical tumors exist, which contain a fatty component or infiltrating appearance and are difficult to diagnose.

Disclosure of interest

The authors declare that they have no conflicts of interest concerning this article.

References

[1] Sibony M, Vieillefond A. Les tumeurs du rein qui ne sont pas des carcinomes à cellules claires. État des lieux en 2008. Ann Pathol 2008;28:381—401.

[2] Delahunt B, Eble JN. Papillary renal cell carcinoma: a clinicopathologic and immunohistochemical study of 105 tumors. Mod Pathol 1997;10:537—44.

[3] Delahunt B, Eble JN, McCredie MR, Bethwaite PB, Stewart JH, Bilous AM. Morphologic typing of papillary renal cell carcinoma: comparison of growth kinetics and patient survival in 66 cases. Hum Pathol 2001;32:590—5.

[4] Amin MB, Tamboli P, Javidan J, Stricker H, de Peralta-Venturina M, Deshpande A, et al. Prognostic impact of histologic subtyping of adult renal epithelial neoplasms: an experience of 405 cases. Am J Surg Pathol 2002;26:281—91.
[5] Moch H, Gasser T, Amin MB, Torhorst J, Sauter G, Mihatsch MJ. Prognostic utility of the recently recommended histologic classification and revised TNM staging system of renal cell carcinoma: a Swiss experience with 588 tumors. Cancer 2000;89:604—14.
[6] Cheville JC, Lohse CM, Zincke H, Weaver AL, Blute ML. Comparisons of outcome and prognostic features among histologic subtypes of renal cell carcinoma. Am J Surg Pathol 2003;27:612—24.
[7] Margulis V, Tamboli P, Matin SF, Swanson DA, Wood CG. Analysis of clinicopathologic predictors of oncologic outcome provides insight into the natural history of surgically managed papillary renal cell carcinoma. Cancer 2008;112:1480—8.
[8] Patard JJ, Leray E, Rioux-Leclercq N, Cindolo L, Ficarra V, Zisman A, et al. Prognostic value of histologic subtypes in renal cell carcinoma: a multicenter experience. J Clin Oncol 2005;23:2763—71.
[9] Beck SD, Patel MI, Snyder ME, Kattan MW, Motzer RJ, Reuter VE, et al. Effect of papillary and chromophobe cell type on disease free survival after nephrectomy for renal cell carcinoma. Ann Surg Oncol 2004;11:71—7.
[10] Herts BR, Coll DM, Novick AC, Obuchowski N, Linnell G, Wirth SL, et al. Enhancement characteristics of papillary renal neoplasms revealed on triphasic helical CT of the kidneys. AJR Am J Roentgenol 2002;178:367—72.
[11] Roy C, Sauer B, Lindner V, Lang H, Saussine C, Jacqmin D. MR imaging of papillary renal neoplasms: potential application for characterization of small renal masses. Eur Radiol 2007;17:193—200.
[12] Bae KT, Heiken JP, Siegel CL, Bennett HF. Renal cysts: is attenuation artifactually increased on contrast-enhanced CT images? Radiology 2000;216:792—6.
[13] Ho VB, Allen SF, Hood MN, Choyke PL. Renal masses: quantitative assessment of enhancement with dynamic MR imaging. Radiology 2002;224:695—700.
[14] Kim JK, Kim TK, Ahn HJ, et al. Differentiation of subtypes of renal cell carcinoma on helical CT scans. AJR Am J Roentgenol 2002;178:1499—506.
[15] Sheir KZ, El-Azab M, Mosbah A, et al. Differentiation of renal cell carcinoma subtypes by multislice computerized tomography. J Urol 2005;174:451—5.
[16] Sun MR, Ngo L, Genega EM, Atkins MB, Finn ME, Rofsky NM, et al. Renal cell carcinoma: dynamic contrast-enhanced MR imaging for differentiation of tumor subtypes — correlation with pathologic findings. Radiology 2009;250(3):793—802.
[17] de Peralta-Venturina M, Moch H, Amin M, et al. Sarcomatoid differentiation in renal cell carcinoma: a study of 101 cases. Am J Surg Pathol 2001;25(3):275—84.
[18] Dyer R, DiSantis DJ, McClennan BL. Simplified imaging approach for evaluation of the solid renal mass in adults. Radiology 2008;247(2):331—43.
[19] Hartman DS, Davidson AJ, Davis Jr CJ, Goldman SM. Infiltrative renal lesions: CT-sonographic-pathologic correlation. AJR Am J Roentgenol 1988;150(5):1061—4.
[20] Pickhardt PJ, Lonergan GJ, Davis Jr CJ, Kashitani N, Wagner BJ, Armed Forces Institute of Pathology. From the archives of the AFIP. Infiltrative renal lesions: radiologic-pathologic correlation. Radiographics 2000;20(1):215—43.
[21] Merran S, Vieillefond A, Peyromaure M, Dupuy C. Renal angiomyolipoma with calcification: CT-pathology correlation. Br J Radiol 2004;77:782—3.
[22] Lesavre A, Correas JM, Merran S, Grenier N, Vieillefond A, Hélénon O. CT of papillary renal cell carcinomas with cholesterol necrosis mimicking angiomyolipomas. AJR Am J Roentgenol 2003;181(1):143—5.
[23] Hélénon O, Chrétien Y, Paraf F, Melki P, Denys A, Moreau JF. Renal cell carcinoma containing fat: demonstration with CT. Radiology 1993;188(2):429—30.
[24] Hélénon O, Merran S, Paraf F, Melki P, Correas JM, Chrétien Y, et al. Unusual fat-containing tumors of the kidney: a diagnostic dilemma. Radiographics 1997;17(1):129—44.
[25] Hayn MH, Cannon Jr GM, Bastacky S, Hrebinko RL. Renal cell carcinoma containing fat without associated calcifications: two case reports and review of literature. Urology 2009;73(2), 443.e5—7.
[26] Bosniak MA. The current radiological approach to renal cysts. Radiology 1986;158:1—10.
[27] Hélénon O, Eiss D, Debrito P, Merran S, Correas JM. How to characterise a solid renal mass: a new classification proposal for a simplified approach. Diagn Interv Imaging 2012;93(4): 232—45.
[28] Israel GM, Bosniak MA. How I do it: evaluating renal masses. Radiology 2005;236(2):441—50.
[29] Herts BR, Paushter DM, Einstein DM, Zepp R, Friedman RA, Obuchowski N. Use of contrast material for spiral CT of the abdomen: comparison of hepatic enhancement and vascular attenuation for three different contrast media at two different delay times. AJR Am J Roentgenol 1995;164: 327—31.
[30] Shinmoto H, Yuasa Y, Tanimoto A, Narimatsu Y, Jinzaki M, Hiramatsu K, et al. Small renal cell carcinoma: MRI with pathologic correlation. J Magn Reson Imaging 1998;8(3): 690—4.
[31] Yoshimitsu K, Kakihara D, Irie H, Tajima T, Nishie A, Asayama Y, et al. Papillary renal carcinoma: diagnostic approach by chemical shift gradient-echo and echo-planar MR imaging. J Magn Reson Imaging 2006;23:339—44.
[32] Amin MB, Corless CL, Renshaw AA, Tickoo SK, Kubus J, Schultz DS. Papillary (chromophil) renal cell carcinoma: histomorphologic characteristics and evaluation of conventional pathologic prognostic parameters in 62 cases. Am J Surg Pathol 1997;21(6):621—35.
[33] Oliva MR, Glickman JN, Zou KH, Teo SY, Mortelé KJ, Rocha MS, et al. Renal cell carcinoma: T1 and T2 signal intensity characteristics of papillary and clear cell types correlated with pathology. AJR Am J Roentgenol 2009;192(6):1524—30.